Supplementary Informatoin for "Quantum Geometry in Quantum Materials"

Jiabin Yu,[1,2] B. Andrei Bernevig,[2,3,4,*] Raquel Queiroz,[5,*]
Enrico Rossi,[6,*] Päivi Törmä,[7,*] and Bohm-Jung Yang[8,9,10,*]

[1]*Department of Physics, University of Florida, Gainesville, FL, USA*
[2]*Department of Physics, Princeton University, Princeton, New Jersey 08544, USA*
[3]*Donostia International Physics Center, P. Manuel de Lardizabal 4, 20018 Donostia-San Sebastian, Spain*
[4]*IKERBASQUE, Basque Foundation for Science, Bilbao, Spain*
[5]*Department of Physics, Columbia University, New York, NY, USA*
[6]*Department of Physics, William & Mary, Williamsburg, Virginia 23187, USA*
[7]*Department of Applied Physics, Aalto University School of Science, FI-00076 Aalto, Finland*
[8]*Department of Physics and Astronomy, Seoul National University, Seoul 08826, Korea*
[9]*Center for Theoretical Physics (CTP), Seoul National University, Seoul 08826, Korea*
[10]*Institute of Applied Physics, Seoul National University, Seoul 08826, Korea*

Appendix A: Quantum geometric tensor (Fubini-Study metric)

1. General Mathematical Formulation

This section contains the formulation of the QGT in mathematical language. We present it here to link to the available mathematical physics literature.

Suppose we have N orthonormal row vectors $u_{n\boldsymbol{k}}$, $n = 1 \dots N$, in a Hilbert space, where $\boldsymbol{k}$ is a vector of generic parameter. The QGT is defined as:

$$[Q_{ij}(\boldsymbol{k})]_{mn} = \partial_{k_i} u^{\dagger}_{m\boldsymbol{k}} \left(1 - \sum_{l=1}^{N} u_{l\boldsymbol{k}} u^{\dagger}_{l\boldsymbol{k}}\right) \partial_{k_j} u_{n\boldsymbol{k}} \ , \tag{A1}$$

where i, j are spatial direction indices. For convenience, we denote $\tilde{u}_{\boldsymbol{k}} = (u_{1\boldsymbol{k}}, u_{2\boldsymbol{k}}, \cdots, u_{N\boldsymbol{k}})$. Using $\tilde{u}_{\boldsymbol{k}}$, the QGT can be expressed compactly :

$$Q_{ij}(\boldsymbol{k}) = \partial_{k_i} \tilde{u}^{\dagger}_{\boldsymbol{k}} \left(\mathbb{1} - \tilde{u}_{\boldsymbol{k}} \tilde{u}^{\dagger}_{\boldsymbol{k}}\right) \partial_{k_j} \tilde{u}_{\boldsymbol{k}} \, . \tag{A2}$$

We use $G_{ij}(\boldsymbol{k})$ to denote $\left[Q_{ij}(\boldsymbol{k}) + Q_{ji}(\boldsymbol{k})\right]/2$, and $g_{ij}(\boldsymbol{k}) = \mathrm{Tr}\left[G_{ij}(\boldsymbol{k})\right]$ is the quantum metric. As the Berry connection is defined by $\boldsymbol{A}(\boldsymbol{k}) = \mathrm{i}\tilde{u}^{\dagger}_{\boldsymbol{k}} \partial_{\boldsymbol{k}} \tilde{u}_{\boldsymbol{k}}$, then the anti-symmetric part of Q_{ij} is proportional to the nonabelian Berry curvature: $\left[Q_{ij}(\boldsymbol{k}) - Q_{ji}(\boldsymbol{k})\right]/2 = -\frac{\mathrm{i}}{2} F_{ij}(\boldsymbol{k}) = -\frac{\mathrm{i}}{2}\left(\partial_{k_i} A_j(\boldsymbol{k}) - \partial_{k_j} A_i(\boldsymbol{k}) - \mathrm{i}[A_i(\boldsymbol{k}), A_j(\boldsymbol{k})]\right)$. The QGT is then

$$Q_{ij}(\boldsymbol{k}) = G_{ij}(\boldsymbol{k}) - \frac{\mathrm{i}}{2} F_{ij}(\boldsymbol{k}) \, , \tag{A3}$$

An important property of G_{ij} is its positive definiteness. Suppose we have several complex vectors $c_i \in \mathbb{C}^n$, we obtain:

$$\begin{aligned} &\sum_{ij} c^{\dagger}_i Q_{ij}(\boldsymbol{k}) c_j \\ &= \sum_{ij} \sum_{l,m=1}^{n} c^{*}_{i,l} \left[Q_{ij}(\boldsymbol{k})\right]_{lm} c_{j,m} \\ &= \left(\sum_i c^{\dagger}_i \partial_{k_i} \tilde{u}^{\dagger}_{\boldsymbol{k}}\right) \left(\mathbb{1} - \tilde{u}_{\boldsymbol{k}} \tilde{u}^{\dagger}_{\boldsymbol{k}}\right) \left(\sum_i \partial_{k_i} \tilde{u}_{\boldsymbol{k}} c_i\right) \\ &= \varphi^{\dagger} \left(\mathbb{1} - \tilde{u}_{\boldsymbol{k}} \tilde{u}^{\dagger}_{\boldsymbol{k}}\right) \varphi \ , \end{aligned} \tag{A4}$$

---

* These authors are listed alphabetically.

where $\varphi = \sum_i \partial_{k_i} \tilde{u}_{\boldsymbol{k}} c_i$. As $\{u_m(\boldsymbol{k})\}$ are orthonormal vectors, the matrix $\left(\mathbb{1} - \tilde{u}_{\boldsymbol{k}} \tilde{u}_{\boldsymbol{k}}^\dagger\right)$ is a projector with eigenvalue 0 or 1. Therefore the scalar product $\varphi^\dagger \left(\mathbb{1} - \tilde{u}_{\boldsymbol{k}} \tilde{u}_{\boldsymbol{k}}^\dagger\right) \varphi$ is non-negative. For the proper choice of complex vectors c_i properly, Eq. (A4) can be used to prove inequalities between the quantum metric and Berry curvature, *i.e.*, the so-called lower bounds.

2. Geometric Interpretation of Quantum Metric

The geometric meaning of the quantum metric is the distance between quantum states. The Bloch wave functions of N bands $\tilde{u}_{\boldsymbol{k}}$ define a map from the Brillouin zone torus to $\mathbb{CP}^{N-1}$. The distance between two points $\boldsymbol{k}$ and $\boldsymbol{k} + d\boldsymbol{k}$ is defined as:

$$d^2(\boldsymbol{k}, \boldsymbol{k} + d\boldsymbol{k}) = \frac{1}{2} \mathrm{Tr} \left(\tilde{u}_{\boldsymbol{k}} \tilde{u}_{\boldsymbol{k}}^\dagger - \tilde{u}_{\boldsymbol{k}+d\boldsymbol{k}} \tilde{u}_{\boldsymbol{k}+d\boldsymbol{k}}^\dagger \right)^2 . \tag{A5}$$

By expanding this equation to the second order we will find $d^2(\boldsymbol{k}, \boldsymbol{k} + d\boldsymbol{k}) = \sum_{ij} g_{ij}(\boldsymbol{k}) dk_i dk_j$ and represents a direct link between the quantum distance and the QGT.

3. Physical Interpretation

Now we focus on the quantum geometry in condensed matter system, where $\boldsymbol{k}$ is the Bloch momentum, and $u_{n\boldsymbol{k}}$ should be replaced by $|u_{n\boldsymbol{k}}\rangle$, which is the periodic part of the Bloch state $|\psi_{n\boldsymbol{k}}\rangle$. The quantum metric is related to the Wannier function localization which is studied in Ref. [1]. Here the Wannier states is the Fourier transformation of the Bloch state:

$$|\boldsymbol{R}n\rangle = \frac{1}{\sqrt{N}} \sum_{\boldsymbol{k}} e^{-i\boldsymbol{k}\cdot\boldsymbol{R}} |\psi_{n\boldsymbol{k}}\rangle \ , \tag{A6}$$

where N here is the number of lattice sites. The Wannier function localization functional can be defined in the Wannier basis:

$$\Omega = \sum_n \left[\langle 0n|\hat{\boldsymbol{r}}^2|0n\rangle - |\langle 0n|\hat{\boldsymbol{r}}|0n\rangle|^2 \right] , \tag{A7}$$

where $\hat{\boldsymbol{r}}$ is the position operator. We now express it in the Bloch basis. Owing to

$$|\psi_{n\boldsymbol{k}}\rangle = e^{i\boldsymbol{k}\cdot\hat{\boldsymbol{r}}} |u_{n\boldsymbol{k}}\rangle \ ,$$

the overlap between the periodic parts of two Bloch functions with different momenta is:

$$\langle u_{m\boldsymbol{k}}|u_{n\boldsymbol{k}+\boldsymbol{q}}\rangle = \langle \psi_{m\boldsymbol{k}}|e^{-i\boldsymbol{q}\cdot\hat{\boldsymbol{r}}}|\psi_{n\boldsymbol{k}+\boldsymbol{q}}\rangle \, . \tag{A8}$$

The right-hand side of this equation is the Bloch states. We can transform it into Wannier states:

$$\langle u_{m\boldsymbol{k}}|u_{n\boldsymbol{k}+\boldsymbol{q}}\rangle = \frac{1}{N} \sum_{\boldsymbol{R}\boldsymbol{R}'} e^{-i\boldsymbol{k}\cdot(\boldsymbol{R}'-\boldsymbol{R})} \langle \boldsymbol{R}'m|e^{-i\boldsymbol{q}\cdot\hat{\boldsymbol{r}}}|\boldsymbol{R}n\rangle e^{i\boldsymbol{q}\cdot\boldsymbol{R}} \ . \tag{A9}$$

The Wannier functions have a discrete translation symmetry along the Bravias lattice:

$$\langle \boldsymbol{R}'m|e^{-i\boldsymbol{q}\cdot\hat{\boldsymbol{r}}}|\boldsymbol{R}n\rangle e^{i\boldsymbol{q}\cdot\boldsymbol{R}} = \langle (\boldsymbol{R}' - \boldsymbol{R})m|e^{-i\boldsymbol{q}\cdot\hat{\boldsymbol{r}}}|0n\rangle \, ,$$

Eq. (A8) becomes

$$\langle u_{m\boldsymbol{k}}|u_{n\boldsymbol{k}+\boldsymbol{q}}\rangle = \sum_{\boldsymbol{R}} e^{-i\boldsymbol{k}\cdot\boldsymbol{R}} \langle \boldsymbol{R}m|e^{-i\boldsymbol{q}\cdot\hat{\boldsymbol{r}}}|0n\rangle \, .$$

We take the first and second-order derivatives of $\boldsymbol{q}$ on both sides of this equation, and then evaluate the result at $q = 0$:

$$\langle u_{m\boldsymbol{k}}|\nabla_{\boldsymbol{k}}|u_{n\boldsymbol{k}}\rangle = -\mathrm{i} \sum_{\boldsymbol{R}} e^{-i\boldsymbol{k}\cdot\boldsymbol{R}} \langle \boldsymbol{R}m|\hat{\boldsymbol{r}}|0n\rangle \tag{A10}$$

$$\langle u_{m\boldsymbol{k}}|\nabla_{\boldsymbol{k}}^2|u_{n\boldsymbol{k}}\rangle = -\sum_{\boldsymbol{R}} e^{-i\boldsymbol{k}\cdot\boldsymbol{R}} \langle \boldsymbol{R}m|\hat{\boldsymbol{r}}^2|0n\rangle \, . \tag{A11}$$

Taking the Fourier transformation

$$\langle \boldsymbol{R}m|\hat{\boldsymbol{r}}|0n\rangle = \mathrm{i}\frac{1}{N}\sum_{\boldsymbol{k}}\langle u_m(\boldsymbol{k})|\nabla_{\boldsymbol{k}}|u_{n\boldsymbol{k}}\rangle e^{i\boldsymbol{k}\cdot\boldsymbol{R}} \tag{A12}$$

$$\langle \boldsymbol{R}m|\hat{\boldsymbol{r}}^2|0n\rangle = -\frac{1}{N}\sum_{\boldsymbol{k}}\langle u_m(\boldsymbol{k})|\nabla^2_{\boldsymbol{k}}|u_{n\boldsymbol{k}}\rangle e^{i\boldsymbol{k}\cdot\boldsymbol{R}}\,. \tag{A13}$$

We divide the localization functional Ω into the following two parts:

$$\begin{aligned}\Omega &= \sum_n \left[\langle 0n|\hat{\boldsymbol{r}}^2|0n\rangle - |\langle 0n|\hat{\boldsymbol{r}}|0n\rangle|^2\right] \\ &= \sum_n \left[\langle 0n|\hat{\boldsymbol{r}}^2|0n\rangle - \sum_{\boldsymbol{R}m}|\langle \boldsymbol{R}m|\hat{\boldsymbol{r}}|0n\rangle|^2\right] + \\ &+ \sum_n \sum_{\boldsymbol{R}m\neq 0n} |\langle \boldsymbol{R}m|\hat{\boldsymbol{r}}|0n\rangle|^2\,,\end{aligned} \tag{A14}$$

We denote the first and second terms in Eq. (A14) by Ω_I and $\tilde{\Omega}$, respectively. $\tilde{\Omega}$ is obviously always non-negative. Using Eq. (A12) and Eq. (A13), Ω_I can be written as the following form:

$$\begin{aligned}\Omega_I = &-\frac{1}{N}\sum_{\boldsymbol{k}}\sum_n \langle u_{n\boldsymbol{k}}|\nabla^2_{\boldsymbol{k}}|u_{n\boldsymbol{k}}\rangle \\ &-\frac{1}{N}\sum_{\boldsymbol{k}}\sum_{nm}\langle u_{m\boldsymbol{k}}|\nabla_{\boldsymbol{k}}u_{n\boldsymbol{k}}\rangle\cdot\langle \nabla_{\boldsymbol{k}}u_{n\boldsymbol{k}}|u_{m\boldsymbol{k}}\rangle\end{aligned} \tag{A15}$$

As $\langle 0n|\hat{\boldsymbol{r}}^2|0n\rangle$ is a real number, we can take complex conjugation and obtain

$$\frac{1}{N}\sum_{\boldsymbol{k}}\left\langle u_{n\boldsymbol{k}}|\nabla^2_{\boldsymbol{k}}u_{n\boldsymbol{k}}\right\rangle = \frac{1}{N}\sum_{\boldsymbol{k}}\left\langle \nabla^2_{\boldsymbol{k}}u_{n\boldsymbol{k}}|u_{n\boldsymbol{k}}\right\rangle\,. \tag{A16}$$

Owign to $\langle u_{n\boldsymbol{k}}|u_{n\boldsymbol{k}}\rangle = 1$, the second order derivative gives $\left\langle u_{n\boldsymbol{k}}|\nabla^2_{\boldsymbol{k}}u_{n\boldsymbol{k}}\right\rangle + \left\langle \nabla^2_{\boldsymbol{k}}u_{n\boldsymbol{k}}|u_{n\boldsymbol{k}}\right\rangle + 2\sum_i \langle \partial_{k_i}u_{n\boldsymbol{k}}|\partial_{k_i}u_{n\boldsymbol{k}}\rangle = 0$. Consequently, we obtain

$$\begin{aligned}&-\frac{1}{N}\sum_{\boldsymbol{k}}\left\langle u_{n\boldsymbol{k}}|\nabla^2_{\boldsymbol{k}}u_{n\boldsymbol{k}}\right\rangle \\ &= -\frac{1}{2}\frac{1}{N}\sum_{\boldsymbol{k}}\left\langle u_{n\boldsymbol{k}}|\nabla^2_{\boldsymbol{k}}u_{n\boldsymbol{k}}\right\rangle - \frac{1}{2}\frac{1}{N}\sum_{\boldsymbol{k}}\left\langle \nabla^2_{\boldsymbol{k}}u_{n\boldsymbol{k}}|u_{n\boldsymbol{k}}\right\rangle \\ &= \frac{1}{N}\sum_{\boldsymbol{k}}\sum_i \langle \partial_{k_i}u_{n\boldsymbol{k}}|\partial_{k_i}u_{n\boldsymbol{k}}\rangle\ .\end{aligned} \tag{A17}$$

We use this to replace the first term in Ω_I:

$$\begin{aligned}\Omega_I &= \frac{1}{N}\sum_{\boldsymbol{k}}\sum_{n,i}\langle \partial_{k_i}u_{n\boldsymbol{k}}|\partial_{k_i}u_{n\boldsymbol{k}}\rangle \\ &\quad -\frac{1}{N}\sum_{\boldsymbol{k}}\sum_{nm,i}\langle \partial_{k_i}u_{n\boldsymbol{k}}|u_{m\boldsymbol{k}}\rangle\langle u_{m\boldsymbol{k}}|\partial_{k_i}u_{n\boldsymbol{k}}\rangle \\ &= \frac{1}{N}\sum_{\boldsymbol{k}}\mathrm{Tr}\left[g(\boldsymbol{k})\right]\end{aligned} \tag{A18}$$

Since the quantum metric is invariant under gauge transformation, Ω_I is gauge invariant. If the integral of $\mathrm{Tr}\left[g(\boldsymbol{k})\right]$ has a nonzero lower bound, the gauge-invariant part of the Wannier function localization functional will also be bounded. Because $\tilde{\Omega}$ is always positive by definition, the lower bound of the gauge invariant part Ω_I is also the lower bound of the functional Ω itself.

Appendix B: Examples of Quantum Geometric Contribution to Spin Stiffness

In this appendix, we provide examples for the quantum geometric contribution to the spin stiffness. Let H_0 be the single-particle Hamiltonian for TBG projected on the active 8 lowest-energy bands, 2 per spin and valley degree of freedom. The Hamiltonian, H_I describing the Coulomb interaction when projected on the active bands of H_0, takes the form of a positive semidefinite Hamiltonian that can be written in the form [2]

$$H_I = \frac{1}{A}\sum_{\boldsymbol{G},\boldsymbol{q}} O_{\boldsymbol{q},\boldsymbol{G}} O_{-\boldsymbol{q},-\boldsymbol{G}} \tag{B1}$$

where A is the sample area, $\{\boldsymbol{G}\}$ are the reciprocal lattice vectors of the moiré lattice, $\{\boldsymbol{q}\}$ are the wave vectors within the moiré BZ and

$$\begin{aligned} O_{\boldsymbol{q},\boldsymbol{G}} =& \sum_{\substack{\boldsymbol{k},m,n,\\ \eta,s}} [V(\boldsymbol{G}+\boldsymbol{q})]^{1/2} M^{\eta}_{m,n}(k,\boldsymbol{q}+\boldsymbol{G}) \\ & \times (\rho^{(\eta)}_{\boldsymbol{k},\boldsymbol{q},m,n,s} - \delta_{\boldsymbol{q},0}\delta_{m,n}/2). \end{aligned} \tag{B2}$$

In Eq. (B2) $m(n) \pm 1$, η, and s are the band, valley, and spin indices, respectively, $V(\boldsymbol{q})$ is the Coulomb interaction, $\rho^{(\eta)}_{\boldsymbol{k},\boldsymbol{q},m,n,s}$ is the density operator in the band basis and $M^{\eta}_{m,n}(k,\boldsymbol{q}+\boldsymbol{G}) = \left\langle u_{\eta,m(\boldsymbol{k}+\boldsymbol{q})} | u_{\eta,n\boldsymbol{k}} \right\rangle$ are the overlap matrices, *form factors*, between the bands' $|u_{\eta,m\boldsymbol{k}}\rangle$ for valley η. The presence of the overlap matrices in the expression of the operators $O_{\boldsymbol{q},\boldsymbol{G}}$ is responsible for quantum geometry terms in the expressions for the dispersion of the excitations.

Starting from H_I we can write the energy $E_G(\boldsymbol{q})$ of the neutral, long wavelength ($q \to 0$), "Goldstone" excitations in terms of the interaction potential and form factors. Up to second order in $\boldsymbol{q}$, $E_G(\boldsymbol{q})$ can be written as:

$$E_G(\boldsymbol{q}) = \frac{1}{2}\sum_{ij} [D_s^{(s)}]_{ij} q_i q_j \tag{B3}$$

The stiffness $[D_s^{(s)}]_{ij}$ can be expressed analytically in some limits.

In Ref. [3], it was shown that in the first chiral limit, the limit in which the interlayer coupling between A sublattices is zero, the form factors take a simple, diagonal, form [3]:

$$M^{(\eta)}_{e_Y}(\boldsymbol{k},\boldsymbol{q}+\boldsymbol{G}) = \alpha_0(\boldsymbol{k},\boldsymbol{q}+\boldsymbol{G})\xi^0\tau^0 + i\xi^y\tau^0\alpha_2(\boldsymbol{k},\boldsymbol{q}+\boldsymbol{G}) \tag{B4}$$

where e_Y is the Euler's class ($C = \pm e_Y = \pm 1$), ξ^i, τ^i are Pauli-matrices acting on the band and valley indices, respectively, and α_i are real functions. In this limit, when $M^{\eta}_{m,n}(\boldsymbol{k},\boldsymbol{q}+\boldsymbol{G})$ for $\boldsymbol{q}=0$ do not depend on $\boldsymbol{k}$, flat metric condition that is valid at, or close to, the first magic angle [4], we have [3]:

$$\begin{aligned} [D_s^{(s)}]_{ij} =& \frac{1}{2A}\sum_{\boldsymbol{k},\boldsymbol{q},\boldsymbol{G}} V(\boldsymbol{G}+\boldsymbol{q}) \\ & \times [\alpha_0(\boldsymbol{k},\boldsymbol{q}+\boldsymbol{G})\partial_{k_i}\partial_{k_j}\alpha_0(\boldsymbol{k},\boldsymbol{q}+\boldsymbol{G}) \\ & + \alpha_2(\boldsymbol{k},\boldsymbol{q}+\boldsymbol{G})\partial_{k_i}\partial_{k_j}\alpha_2(\boldsymbol{k},\boldsymbol{q}+\boldsymbol{G}) \\ & + 2\partial_{k_i}\alpha_0(\boldsymbol{k},\boldsymbol{q}+\boldsymbol{G})\partial_{k_j}\alpha_0(\boldsymbol{k},\boldsymbol{q}+\boldsymbol{G}) \\ & + 2\partial_{k_i}\alpha_2(\boldsymbol{k},\boldsymbol{q}+\boldsymbol{G})\partial_{k_j}\alpha_2(\boldsymbol{k},\boldsymbol{q}+\boldsymbol{G})] \end{aligned} \tag{B5}$$

from which the explicit relation between the spin stiffness and the metric of the bands can be extracted. Within mean-field theory, and a single-mode approximation, Ref. [5] obtained an explicit, but approximate, relation between the spin-wave stiffness of the spin-and-valley maximally polarized sate at filling $\nu = 3$ and the quantum geometric properties of the highest-energy filled band:

$$[D_s^{(s)}]_{ij} = \frac{1}{AN_{MC}}\delta_{ij}\sum_{\boldsymbol{k}\boldsymbol{q},l,m} \Omega^2_{\boldsymbol{k}} \exp(-q_l g_{lm} q_m), \tag{B6}$$

where N_{MC} is the number of moiré cells within A.

For the case of saturated ferromagnetism, using the variational approach, the authors of Ref. [6] found that in the strongly correlated limit,

$$[D_s^{(s)}]_{ij} = \frac{1}{N_c N_{\rm occ}}\sum_{\boldsymbol{k}}^{N_c}\sum_{n}^{N_{\rm occ}} [\partial_{k_i}\partial_{k_j}\epsilon_{n\boldsymbol{k}} + 2\Delta(\boldsymbol{k})g_{ij}(\boldsymbol{k})], \tag{B7}$$

where $\epsilon_{n\boldsymbol{k}}$ are the eigenvalues of the single-particle Hamiltonian, N_c is the number of unit cells in the sample, and $N_{\rm occ}$ is the number of occupied states per unit cell. Notice that in this approximation, the occupied (and unoccupied) bands are degenerate, so $g_{ij}(\boldsymbol{k})$ in Eq. (B6) is the Abelian (minimal) quantum metric.

Equations (B5),(B6),(B7) exemplify, for specific cases, the role of the bands' quantum geometry in determining the spin, or pseudospin, stiffness and therefore the dispersion of the associated Goldstone modes.

Appendix C: Quantum Geometry and Electron-Phonon Coupling

In this appendix, we provide additional details on the Gaussian approximation (GA) based on Ref. [7] and use it to illustrate how quantum geometry contributes to the EPC.

Under the tight-binding approximation and Frohlich two-center approximation [8], the non-interacting electron Hamiltonian and the EPC Hamiltonian are directly given by the smooth hopping function $t(\boldsymbol{r})$, which satisfies $[t(\boldsymbol{r})]^* = t(-\boldsymbol{r})$ to ensure Hermiticity.

Here, $t(\boldsymbol{r})$ does not carry any orbital, sublattice, or spin indices, as we focus on one type of atom and one spinless s orbital per atom, though more than one atom per unit cell may be present.

Using the hopping function, the electron Hamiltonian (without the Coulomb interaction) that accounts for atomic motions reads

$$\begin{aligned} H_{el+ion-motions} = &\sum_{\boldsymbol{R\tau},\boldsymbol{R'\tau'}} c^\dagger_{\boldsymbol{R+\tau}} c_{\boldsymbol{R'+\tau'}} \\ &\times t(\boldsymbol{R}+\boldsymbol{\tau}+\boldsymbol{u}_{\boldsymbol{R+\tau}}-\boldsymbol{R'}-\boldsymbol{\tau'}-\boldsymbol{u}_{\boldsymbol{R'+\tau'}}) \ , \end{aligned} \tag{C1}$$

where $\boldsymbol{R}$ labels the lattice point, $\boldsymbol{\tau}$ labels the positions of the sublattices in the $\boldsymbol{R}=0$ unit cell, $c^\dagger_{\boldsymbol{R+\tau}}$ creates an electron in the spinless s orbital at $\boldsymbol{R}+\boldsymbol{\tau}$, and $\boldsymbol{u}_{\boldsymbol{R+\tau}}$ denotes the displacement of the atom at $\boldsymbol{R}+\boldsymbol{\tau}$.

Since the hopping function generally decays exponentially as $|\boldsymbol{r}|$ increases, $t(\boldsymbol{R}+\boldsymbol{\tau}+\boldsymbol{u}_{\boldsymbol{R+\tau}}-\boldsymbol{R'}-\boldsymbol{\tau'}-\boldsymbol{u}_{\boldsymbol{R'+\tau'}})$ can be expanded in a series of $(\boldsymbol{u}_{\boldsymbol{R+\tau}}-\boldsymbol{u}_{\boldsymbol{R'+\tau'}})$.

The zeroth-order term yields the non-interacting electron Hamiltonian under the tight-binding approximation:

$$H_{el} = \sum_{\boldsymbol{R\tau},\boldsymbol{R'\tau'}} t(\boldsymbol{R}+\boldsymbol{\tau}-\boldsymbol{R'}-\boldsymbol{\tau'}) c^\dagger_{\boldsymbol{R+\tau}} c_{\boldsymbol{R'+\tau'}} \ , \tag{C2}$$

and the first-order term is the leading order term for EPC, given by

$$\begin{aligned} H_{el-ph} = &\sum_{\boldsymbol{R\tau},\boldsymbol{R'\tau'}} \sum_{\alpha_{\boldsymbol{\tau}}\alpha'_{\boldsymbol{\tau'}}} c^\dagger_{\boldsymbol{R+\tau},\alpha_{\boldsymbol{\tau}}} c_{\boldsymbol{R'+\tau'},\alpha'_{\boldsymbol{\tau'}}} \\ &\times (\boldsymbol{u}_{\boldsymbol{R+\tau}}-\boldsymbol{u}_{\boldsymbol{R'+\tau'}}) \cdot \nabla_{\boldsymbol{r}} t(\boldsymbol{r})|_{\boldsymbol{r}=\boldsymbol{R+\tau}-\boldsymbol{R'}-\boldsymbol{\tau'}} \ . \end{aligned} \tag{C3}$$

Higher-order terms are typically neglected.

The GA assumes that the hopping function has a Gaussian form:

$$t(\boldsymbol{r}) = t_0 \exp\left(\gamma \frac{r^2}{2}\right) \ , \tag{C4}$$

where $r=|\boldsymbol{r}|$, and $\gamma<0$ is determined by the standard deviation of the Gaussian function. As a result, we have

$$\nabla_{\boldsymbol{r}} t(\boldsymbol{r}) = \gamma \boldsymbol{r} t(\boldsymbol{r}) \ . \tag{C5}$$

Eq. (C5) converts the spatial derivative to the position vector in the EPC Hamiltonian (Eq. (C3)), along with an additional factor of γ. To better understand how this conversion connects the EPC Hamiltonian to the electron Hamiltonian, we transform the Hamiltonian to momentum space. Specifically, the Fourier transformation rule for the basis states reads

$$\begin{aligned} c^\dagger_{\boldsymbol{k},\boldsymbol{\tau}} &= \frac{1}{\sqrt{N}} \sum_{\boldsymbol{R}} e^{\mathrm{i}\boldsymbol{k}\cdot(\boldsymbol{R}+\boldsymbol{\tau})} c^\dagger_{\boldsymbol{R+\tau}} \\ u_{\boldsymbol{q\tau}i} &= \frac{1}{\sqrt{N}} \sum_{\boldsymbol{R}} e^{-\mathrm{i}\boldsymbol{q}\cdot(\boldsymbol{R}+\boldsymbol{\tau})} u_{\boldsymbol{R+\tau},i} \ , \end{aligned} \tag{C6}$$

from which we obtain

$$u^\dagger_{\boldsymbol{q}\boldsymbol{\tau}i} = u_{-\boldsymbol{q}\boldsymbol{\tau}i} \ . \tag{C7}$$

For the electron Hamiltonian,

$$H_{el} = \sum_{\boldsymbol{k}}^{1\mathrm{BZ}} c^\dagger_{\boldsymbol{k}} h(\boldsymbol{k}) c_{\boldsymbol{k}} = \sum_{\boldsymbol{k}}^{1\mathrm{BZ}} \sum_n \epsilon_{n\boldsymbol{k}} \gamma^\dagger_{\boldsymbol{k},n} \gamma_{\boldsymbol{k},n} \ , \tag{C8}$$

where $c^\dagger_{\boldsymbol{k}} = (..., c^\dagger_{\boldsymbol{k},\boldsymbol{\tau}}, ...)$,

$$[h(\boldsymbol{k})]_{\boldsymbol{\tau}\boldsymbol{\tau}'} = \sum_{\boldsymbol{R}} t(\boldsymbol{R} + \boldsymbol{\tau} - \boldsymbol{\tau}') e^{-\mathrm{i}\boldsymbol{k}\cdot(\boldsymbol{R}+\boldsymbol{\tau}-\boldsymbol{\tau}')} \ , \tag{C9}$$

$$h(\boldsymbol{k}) U_{n\boldsymbol{k}} = \epsilon_{n\boldsymbol{k}} U_{n\boldsymbol{k}} \ , \tag{C10}$$

and $\gamma^\dagger_{\boldsymbol{k},n} = c^\dagger_{\boldsymbol{k}} U_{n\boldsymbol{k}}$. Under the tight-binding approximation, the term "quantum geometry" (or band geometry) typically refers to the momentum dependence of

$$P_{n\boldsymbol{k}} = U_{n\boldsymbol{k}} U^\dagger_{n\boldsymbol{k}} \ , \tag{C11}$$

and we will particularly use the quantum metric

$$\begin{aligned} g_{n,ij}(\boldsymbol{k}) &= \frac{1}{2} \mathrm{Tr} \left[\partial_{k_i} P_{n\boldsymbol{k}} \partial_{k_j} P_{n\boldsymbol{k}} \right] \\ &= \frac{1}{2} \mathrm{Tr} \left[\partial_{k_i} P_{n\boldsymbol{k}} P_{n\boldsymbol{k}} \partial_{k_j} P_{n\boldsymbol{k}} \right] + (i \leftrightarrow j) \ . \end{aligned} \tag{C12}$$

For the EPC in momentum space, we have

$$\begin{aligned} &H_{el-ph} \\ &= \frac{1}{\sqrt{N}} \sum_{\boldsymbol{k}_1}^{1\mathrm{BZ}} \sum_{\boldsymbol{k}_2}^{1\mathrm{BZ}} \sum_{\boldsymbol{\tau},i} c^\dagger_{\boldsymbol{k}_1} \left[\chi_{\boldsymbol{\tau}} f_i(\boldsymbol{k}_2) - f_i(\boldsymbol{k}_1) \chi_{\boldsymbol{\tau}} \right] c_{\boldsymbol{k}_2} u^\dagger_{\boldsymbol{k}_2-\boldsymbol{k}_1,\boldsymbol{\tau},i} \ , \end{aligned} \tag{C13}$$

where

$$[\chi_{\boldsymbol{\tau}}]_{\boldsymbol{\tau}_1\boldsymbol{\tau}_2} = \delta_{\boldsymbol{\tau},\boldsymbol{\tau}_1} \delta_{\boldsymbol{\tau}_1\boldsymbol{\tau}_2} \tag{C14}$$

is the projection matrix onto the $\boldsymbol{\tau}$ sublattice,

$$[f_i(\boldsymbol{k})]_{\boldsymbol{\tau}_1\boldsymbol{\tau}_2} = \sum_{\boldsymbol{R}} e^{-\mathrm{i}\boldsymbol{k}\cdot(\boldsymbol{R}+\boldsymbol{\tau}_1-\boldsymbol{\tau}_2)} \ \partial_{r_i} t(\boldsymbol{r})|_{\boldsymbol{r}=\boldsymbol{R}+\boldsymbol{\tau}_1-\boldsymbol{\tau}_2} \ , \tag{C15}$$

and $i = x, y, z$ labels the spatial direction. It is clear from Eq. (C13) that the form of the EPC Hamiltonian is governed by $f_i(\boldsymbol{k})$, which we focus on below.

Using Eq. (C5), we find that the EPC term $f_i(\boldsymbol{k})$ relates to the electron matrix Hamiltonian $h(\boldsymbol{k})$ as

$$[f_i(\boldsymbol{k})]_{\boldsymbol{\tau}_1\boldsymbol{\tau}_2} = \mathrm{i}\gamma \partial_{k_i} [h(\boldsymbol{k})]_{\boldsymbol{\tau}_1\boldsymbol{\tau}_2} \ , \tag{C16}$$

which means that

$$f_i(\boldsymbol{k}) = \mathrm{i}\gamma \partial_{k_i} h(\boldsymbol{k}) \ . \tag{C17}$$

We refer to Eq. (C17) as the Gaussian form of the EPC.

The Gaussian form of the EPC allows us to define the energetic and geometric components of the EPC. Note that the electron matrix Hamiltonian contains information about both the bands and the projection matrix, i.e.,

$$h(\boldsymbol{k}) = \sum_n \epsilon_{n\boldsymbol{k}} P_{n\boldsymbol{k}} \ , \tag{C18}$$

where the projection matrix $P_{n\boldsymbol{k}}$ is defined in Eq. (C11). Then, we have

$$f_i(\boldsymbol{k}) = \mathrm{i}\gamma\partial_{k_i} h(\boldsymbol{k}) = f_i^E(\boldsymbol{k}) + f^{geo}(\boldsymbol{k}) \ , \tag{C19}$$

where

$$f_i^E(\boldsymbol{k}) = \mathrm{i}\gamma \sum_n \partial_{k_i}\epsilon_{n\boldsymbol{k}} P_{n\boldsymbol{k}} \tag{C20}$$

is the energetic component of the EPC, which vanishes if all electron bands are exactly flat, and

$$f_i^{geo}(\boldsymbol{k}) = \mathrm{i}\gamma \sum_n \epsilon_{n\boldsymbol{k}}\partial_{k_i} P_{n\boldsymbol{k}} \tag{C21}$$

is the geometric component of the EPC, as $f_i^{geo}(\boldsymbol{k})$ depends on the geometric properties of the Bloch eigenvector $U_{n\boldsymbol{k}}$ (i.e., the momentum dependence of $P_{n\boldsymbol{k}}$). In the one-band case (i.e., with only one atom per unit cell), $f_i^{geo}(\boldsymbol{k})$ must vanish since $P_{n\boldsymbol{k}} = 1$ is independent of momentum (n can only take one value in the one-band case), while $f_i^E(\boldsymbol{k})$ can still be nonzero since the energy band can still vary with momentum.

The key quantity we study is the dimensionless EPC constant λ [9], which is given by

$$\lambda = \frac{2}{N} D(\mu) \frac{1}{\langle\omega^2\rangle} \langle\Gamma\rangle \ , \tag{C22}$$

where μ is the chemical potential, $D(\mu)$ is the electron density of states at μ, and $\langle\omega^2\rangle$ is the mean-squared phonon frequency as defined in Ref. [9]. The EPC matrix element $\Gamma_{nn'}(\boldsymbol{k},\boldsymbol{k}')$ is defined by

$$\begin{aligned}\Gamma_{nn'}(\boldsymbol{k},\boldsymbol{k}') = \frac{1}{2m}\sum_{\boldsymbol{\tau},i} \mathrm{Tr}\left\{P_{n\boldsymbol{k}}\left[\chi_{\boldsymbol{\tau}} f_i(\boldsymbol{k}') - f_i(\boldsymbol{k})\chi_{\boldsymbol{\tau}}\right]\right. \\ \left.\times P_{n'\boldsymbol{k}'}\left[\chi_{\boldsymbol{\tau}} f_i(\boldsymbol{k}) - f_i(\boldsymbol{k}')\chi_{\boldsymbol{\tau}}\right]\right\} \ ,\end{aligned} \tag{C23}$$

where m is the atomic mass, and

$$\langle\Gamma\rangle = \frac{\sum_{\boldsymbol{k},\boldsymbol{k}'}^{1\mathrm{BZ}}\sum_{n,n'}\delta\left(\mu-\epsilon_{n\boldsymbol{k}}\right)\delta\left(\mu-\epsilon_{n'\boldsymbol{k}'}\right)\Gamma_{nn'}(\boldsymbol{k},\boldsymbol{k}')}{\sum_{\boldsymbol{k},\boldsymbol{k}'}^{1\mathrm{BZ}}\sum_{n,n'}\delta\left(\mu-\epsilon_{n\boldsymbol{k}}\right)\delta\left(\mu-\epsilon_{n'\boldsymbol{k}'}\right)} \ . \tag{C24}$$

As discussed in Ref. [7], we will focus on $\langle\Gamma\rangle$ and treat $\langle\omega^2\rangle$ as a parameter determined by first-principles calculations, primarily because $\langle\omega^2\rangle$ can be well-approximated by the frequency of specific phonon modes in graphene and MgB_2 [7]. By combining Eq. (C23) with Eq. (C19), we can express

$$\Gamma_{nn'}(\boldsymbol{k},\boldsymbol{k}') = \Gamma_{nn'}^{E-E}(\boldsymbol{k},\boldsymbol{k}') + \Gamma_{nn'}^{geo-geo}(\boldsymbol{k},\boldsymbol{k}') + \Gamma_{nn'}^{E-geo}(\boldsymbol{k},\boldsymbol{k}') \ , \tag{C25}$$

where

$$\begin{aligned}\Gamma_{nn'}^{E-E}(\boldsymbol{k},\boldsymbol{k}') &= \frac{1}{2m}\sum_{\boldsymbol{\tau},i}\mathrm{Tr}\left\{P_{n\boldsymbol{k}}\left[\chi_{\boldsymbol{\tau}} f_i^E(\boldsymbol{k}') - f_i^E(\boldsymbol{k})\chi_{\boldsymbol{\tau}}\right]\right. \\ &\quad\left.\times\ P_{n'\boldsymbol{k}'}\left[\chi_{\boldsymbol{\tau}} f_i^E(\boldsymbol{k}) - f_i^E(\boldsymbol{k}')\chi_{\boldsymbol{\tau}}\right]\right\} \\ \Gamma_{nn'}^{geo-geo}(\boldsymbol{k},\boldsymbol{k}') &= \frac{1}{2m}\sum_{\boldsymbol{\tau},i}\mathrm{Tr}\left\{P_{n\boldsymbol{k}}\left[\chi_{\boldsymbol{\tau}} f_i^{geo}(\boldsymbol{k}') - f_i^{geo}(\boldsymbol{k})\chi_{\boldsymbol{\tau}}\right]\right. \\ &\quad\left.\times\ P_{n'\boldsymbol{k}'}\left[\chi_{\boldsymbol{\tau}} f_i^{geo}(\boldsymbol{k}) - f_i^{geo}(\boldsymbol{k}')\chi_{\boldsymbol{\tau}}\right]\right\} \\ \Gamma_{nn'}^{E-geo}(\boldsymbol{k},\boldsymbol{k}') &= \frac{1}{2m}\sum_{\boldsymbol{\tau},i}\mathrm{Tr}\left\{P_{n\boldsymbol{k}}\left[\chi_{\boldsymbol{\tau}} f_i^E(\boldsymbol{k}') - f_i^E(\boldsymbol{k})\chi_{\boldsymbol{\tau}}\right]\right. \\ &\quad\left.\times\ P_{n'\boldsymbol{k}'}\left[\chi_{\boldsymbol{\tau}} f_i^{geo}(\boldsymbol{k}) - f_i^{geo}(\boldsymbol{k}')\chi_{\boldsymbol{\tau}}\right]\right\} + c.c. \ .\end{aligned} \tag{C26}$$

By defining

$$\langle\Gamma\rangle^X = \frac{\sum_{\boldsymbol{k},\boldsymbol{k}'}^{1\mathrm{BZ}}\sum_{n,n'}\delta\left(\mu-\epsilon_{n\boldsymbol{k}}\right)\delta\left(\mu-\epsilon_{n'\boldsymbol{k}'}\right)\Gamma_{nn'}^X(\boldsymbol{k},\boldsymbol{k}')}{\sum_{\boldsymbol{k},\boldsymbol{k}'}^{1\mathrm{BZ}}\sum_{n,n'}\delta\left(\mu-\epsilon_{n\boldsymbol{k}}\right)\delta\left(\mu-\epsilon_{n'\boldsymbol{k}'}\right)} \tag{C27}$$

for $X = E-E,\ geo-geo,\ E-geo$, we arrive at

$$\lambda = \lambda_E + \lambda_{geo} + \lambda_{E-geo} \ , \tag{C28}$$

where

$$\lambda_E = \frac{2}{N} D(\mu) \frac{1}{\langle \omega^2 \rangle} \langle \Gamma \rangle^{E-E} \tag{C29}$$

is the energetic contribution to λ as it depends only on f_i^E and not on f_i^{geo},

$$\lambda_{geo} = \frac{2}{N} D(\mu) \frac{1}{\langle \omega^2 \rangle} \langle \Gamma \rangle^{geo-geo} \tag{C30}$$

is the geometric contribution to λ as it depends only on f_i^{geo} and not on f_i^E, and

$$\lambda_{E-geo} = \frac{2}{N} D(\mu) \frac{1}{\langle \omega^2 \rangle} \langle \Gamma \rangle^{E-geo} \tag{C31}$$

is the cross-term contribution to λ as it depends on both f_i^{geo} and f_i^E.

We now further examine the expressions of $\langle \Gamma \rangle^{geo-geo}$ and λ_{geo}. We can split $\langle \Gamma \rangle^{geo-geo}$ into two parts:

$$\langle \Gamma \rangle^{geo-geo} = \langle \Gamma \rangle^{geo-geo,2} + \langle \Gamma \rangle^{geo-geo,1} \ , \tag{C32}$$

where

$$\begin{aligned}
\langle \Gamma \rangle^{geo-geo,1} &= -\frac{1}{D^2(\mu)} \sum_{\boldsymbol{\tau},i} \frac{1}{m} \sum_{\boldsymbol{k}_1,\boldsymbol{k}_2}^{1\mathrm{BZ}} \sum_{n,m} \delta\left(\mu - \epsilon_{n\boldsymbol{k}_1}\right) \\
&\times \delta\left(\mu - \epsilon_{m\boldsymbol{k}_2}\right) \mathrm{Tr}\left[f_i^{geo}(\boldsymbol{k}_1) P_{n\boldsymbol{k}_1} f_i^{geo}(\boldsymbol{k}_1) \chi_{\boldsymbol{\tau}} P_{m\boldsymbol{k}_2} \chi_{\boldsymbol{\tau}} \right] \\
\langle \Gamma \rangle^{geo-geo,2} &= \frac{1}{D^2(\mu)} \frac{1}{2} \frac{1}{m} \sum_{\boldsymbol{\tau},i} \\
&\times \mathrm{Tr}\left[\left(\sum_{\boldsymbol{k}_1}^{1\mathrm{BZ}} \sum_n \delta\left(\mu - \epsilon_{n\boldsymbol{k}_1}\right) \chi_{\boldsymbol{\tau}} f_i^{geo}(\boldsymbol{k}_1) P_{n\boldsymbol{k}_1} \right)^2 \right] + c.c. \ .
\end{aligned} \tag{C33}$$

Similarly, λ_{geo} can be decomposed into two parts:

$$\lambda_{geo} = \lambda_{geo,1} + \lambda_{geo,2} \ , \tag{C34}$$

where

$$\lambda_{geo,1/2} = \frac{2}{N} D(\mu) \frac{1}{\langle \omega^2 \rangle} \langle \Gamma \rangle^{geo-geo,1/2} \ . \tag{C35}$$

For convenience in illustrating the explicit geometric dependence, we re-write $\langle \Gamma \rangle^{geo-geo,1/2}$. $\langle \Gamma \rangle^{geo-geo,1}$ can be re-written as

$$\begin{aligned}
\langle \Gamma \rangle^{geo-geo,1} &= \frac{\gamma^2}{D(\mu)} \sum_i \frac{1}{m} \sum_{\boldsymbol{k}}^{1\mathrm{BZ}} \sum_{n,n_1,n_2} \delta\left(\mu - \epsilon_{n\boldsymbol{k}}\right) \\
&\times \epsilon_{n_1\boldsymbol{k}} \epsilon_{n_2\boldsymbol{k}} \mathrm{Tr}\left[\partial_{k_i} P_{n_1\boldsymbol{k}} P_{n\boldsymbol{k}} \partial_{k_i} P_{n_2\boldsymbol{k}} M \right] \ ,
\end{aligned} \tag{C36}$$

where

$$\begin{aligned}
M &= \frac{1}{D(\mu)} \sum_{\boldsymbol{\tau}} \sum_m \sum_{\boldsymbol{k}_2}^{1\mathrm{BZ}} \delta\left(\mu - \epsilon_{m\boldsymbol{k}_2}\right) \chi_{\boldsymbol{\tau}} P_{m\boldsymbol{k}_2} \chi_{\boldsymbol{\tau}} \\
&= \sum_{\boldsymbol{\tau}} a_{\boldsymbol{\tau}} \chi_{\boldsymbol{\tau}} \ ,
\end{aligned} \tag{C37}$$

and

$$a_{\boldsymbol{\tau}} = \frac{1}{D(\mu)} \sum_{m} \sum_{\boldsymbol{k}_2}^{1\mathrm{BZ}} \delta\left(\mu - \epsilon_{m\boldsymbol{k}_2}\right) \left[P_{m\boldsymbol{k}_2}\right]_{\boldsymbol{\tau}\boldsymbol{\tau}} \tag{C38}$$

In the following, we consider the two-band case (i.e., a system with only two electron bands) for clearer illustration of the explicit geometric dependence.

For $\lambda_{geo,1}$, we have

$$\lambda_{geo,1} = \frac{2\Omega\gamma^2}{(2\pi)^3 m \langle\omega^2\rangle} \sum_{n,i,\boldsymbol{\tau}} \int_{FS_n} d\sigma_{\boldsymbol{k}} \frac{\Delta E^2(\boldsymbol{k})}{|\nabla_{\boldsymbol{k}}\epsilon_{n\boldsymbol{k}}|} a_{\boldsymbol{\tau}} \left[g_{n,\boldsymbol{\tau},ii}(\boldsymbol{k})\right]_{ii} \ , \tag{C39}$$

where $\Delta E(\boldsymbol{k}) = |E_2(\boldsymbol{k}) - E_1(\boldsymbol{k})|$,

$$\left[g_{n,\boldsymbol{\tau}}(\boldsymbol{k})\right]_{ij} = \frac{1}{2} \mathrm{Tr}\left[\partial_{k_i} P_{n\boldsymbol{k}} P_{n\boldsymbol{k}} \partial_{k_j} P_{n\boldsymbol{k}} \chi_{\boldsymbol{\tau}}\right] + (i \leftrightarrow j) \ , \tag{C40}$$

and $a_{\boldsymbol{\tau}}$ is defined in Eq. (C38). As discussed in Ref. [7], $g_{n,\boldsymbol{\tau}}(\boldsymbol{k})$ is an orbital-selective quantum metric, as it is defined by inserting the projection matrix $\chi_{\boldsymbol{\tau}}$ into the original definition of the quantum metric. Therefore, in the two-band case, $\lambda_{geo,1}$ directly depends on the linear combination of the orbital-selective quantum metric.

We can further simplify $\lambda_{geo,2}$ to

$$\begin{aligned} \lambda_{geo,2} = & \frac{N\gamma^2}{mD(\mu)\langle\omega^2\rangle} \sum_{\boldsymbol{\tau},i} \\ & \times \left(\frac{\Omega}{(2\pi)^3} \sum_{n} \int_{FS_n} d\sigma_{\boldsymbol{k}} \frac{\Delta E(\boldsymbol{k})}{|\nabla_{\boldsymbol{k}}\epsilon_{n\boldsymbol{k}}|} \mathcal{A}_{i,n,\boldsymbol{\tau}}(\boldsymbol{k}) \right)^2 + c.c. \ , \end{aligned} \tag{C41}$$

where

$$\boldsymbol{\mathcal{A}}_{n,\boldsymbol{\tau}}(\boldsymbol{k}) = \mathrm{Tr}\left[\chi_{\boldsymbol{\tau}} \nabla_{\boldsymbol{k}} P_{n\boldsymbol{k}} P_{n\boldsymbol{k}}\right] \tag{C42}$$

is an orbital-selective complex vector field. Thus, the explicit geometric dependence in $\lambda_{geo,2}$ arises from the orbital-selective complex vector field.

Finally, in the two-band case, we can also explicitly derive the geometric dependence of λ_{E-geo}, which is given by

$$\begin{aligned} \lambda_{E-geo} = & \frac{\Omega}{(2\pi)^3} \frac{4\gamma^2}{m\langle\omega^2\rangle} \sum_{n} \int_{FS_n} d\sigma_{\boldsymbol{k}} \frac{\Delta E(\boldsymbol{k})}{|\nabla_{\boldsymbol{k}}\epsilon_{n\boldsymbol{k}}|} (-1)^n \\ & \times \sum_{\boldsymbol{\tau},i} \mathrm{Re}[\mathcal{A}_{\boldsymbol{\tau},n,i}(\boldsymbol{k})] \left(\partial_{k_i}\epsilon_{n\boldsymbol{k}} a_{\boldsymbol{\tau}} - b_{\boldsymbol{\tau},i}\right) \ , \end{aligned} \tag{C43}$$

where $a_{\boldsymbol{\tau}}$ is defined in Eq. (C38), $\mathcal{A}_{\boldsymbol{\tau},n,i}(\boldsymbol{k})$ is the orbital-selective complex vector field in Eq. (C42), and

$$b_{\boldsymbol{\tau},i} = \frac{1}{D(\mu)} \sum_{\boldsymbol{k}'}^{1\mathrm{BZ}} \sum_{n'} \delta\left(\mu - \epsilon_{n'\boldsymbol{k}'}\right) \mathrm{Tr}\left[\partial_{k'_i}\epsilon_{n'\boldsymbol{k}'} P_{n'\boldsymbol{k}'} \chi_{\boldsymbol{\tau}}\right] \ . \tag{C44}$$

Thus, we see that the explicit geometric quantity in λ_{E-geo} is again the orbital-selective complex vector field, similar to $\lambda_{geo,2}$.

Appendix D: Quantum Geometry of Nearly Flat Chern Bands

In this appendix, we will compute the quantum metric of the nearly flat Chern bands of the two-band model in Ref. [10], which was used in Ref. [11] to demonstrate FCIs. The model is defined on the square lattice with lattice constant set to 1; the matrix Hamiltonian in the momentum space reads

$$h(\boldsymbol{k}) = \begin{pmatrix} m(\boldsymbol{k}) & r(\boldsymbol{k}) \\ r^*(\boldsymbol{k}) & -m(\boldsymbol{k}) \end{pmatrix} \ , \tag{D1}$$

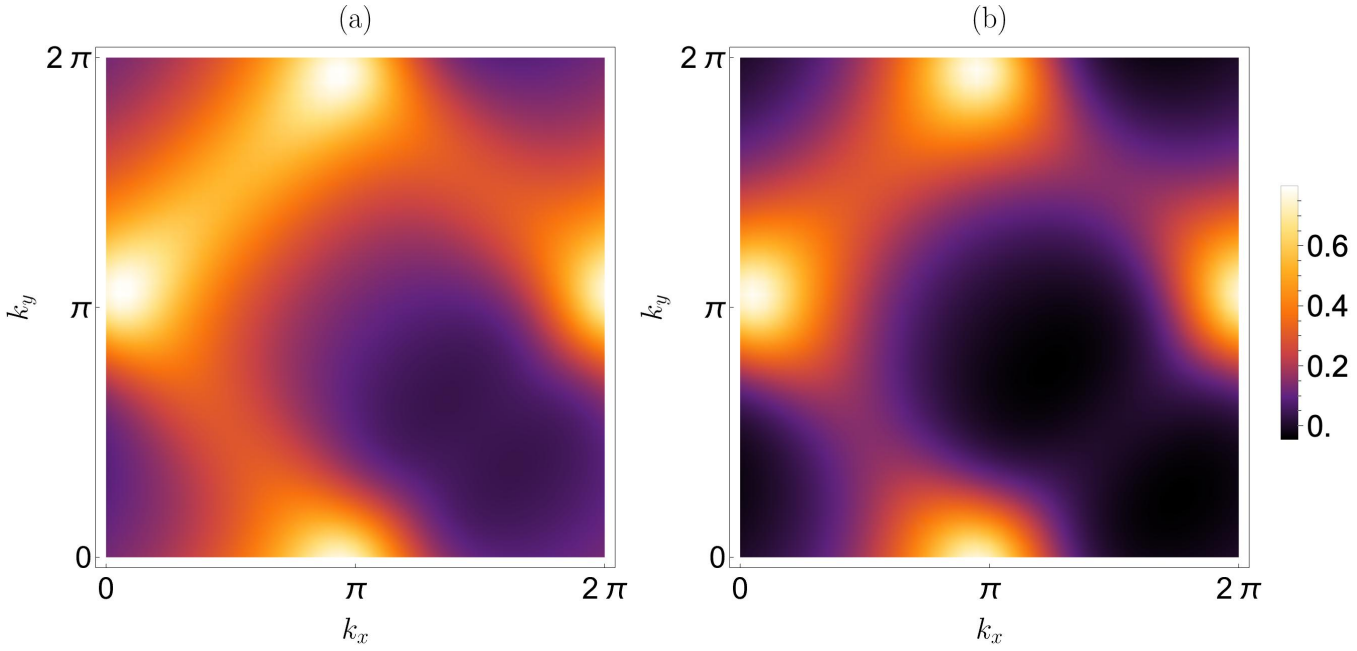

FIG. 1. The plots of the trace of quantum metric ($\mathrm{Tr}[g(\boldsymbol{k})]$) and the Berry curvature of the lower band of the model in Eq. (D1) in (a) and (b), respectively.

where

$$m(\boldsymbol{k}) = 2t_2[\cos(k_x) - \cos(k_y)] + M \ , \tag{D2}$$

and

$$r(\boldsymbol{k}) = t_1 e^{\mathrm{i}\phi}\left[1 + e^{\mathrm{i}(k_y - k_x)}\right] + t_1 e^{-\mathrm{i}\phi}\left[e^{\mathrm{i}k_y} + e^{-\mathrm{i}k_x}\right] \ . \tag{D3}$$

As discussed in Ref. [11], clear numerical evidence of the FCIs can be found for $t_2 = (2-\sqrt{2})/2t_1 > 0$, $\phi = \pi/4$, and $M = 0$, when (i) we consider the fractional fillings of the lower band and (ii) we artificially flatten the dispersion of the lower band. Clearly, flattening the dispersion is to minic the exact flatness of the Landau level. One the other hand, as shown in Fig. 1, the quantum metric and Berry curvature of the lower band have considerable fluctuations, which are not that close to the uniform ones in Landau levels. In particular, the integration over $\mathrm{Tr}[g(\boldsymbol{k})]$, *i.e.*, $\frac{1}{2\pi}\int d^2k\,\mathrm{Tr}[g(\boldsymbol{k})]$, is 1.71 which is not that close to the Chern number 1 of that band. Nevertheless, FCIs can still exist despite the fluctuations of the quantum geometry demonstrates.

[1] N. Marzari and D. Vanderbilt, Maximally localized generalized Wannier functions for composite energy bands, Physical Review B **56**, 12847 (1997), cond-mat/9707145.

[2] B. A. Bernevig, Z.-D. Song, N. Regnault, and B. Lian, Twisted bilayer graphene III. Interacting Hamiltonian and exact symmetries, Physical Review B **103**, 205413 (2021), arXiv:2009.12376 [cond-mat].

[3] B. A. Bernevig, B. Lian, A. Cowsik, F. Xie, N. Regnault, and Z.-D. Song, Twisted bilayer graphene. V. Exact analytic many-body excitations in Coulomb Hamiltonians: Charge gap, Goldstone modes, and absence of Cooper pairing, Physical Review B **103**, 205415 (2021).

[4] B. A. Bernevig, Z.-D. Song, N. Regnault, and B. Lian, Twisted bilayer graphene I. Matrix elements, approximations, perturbation theory and a $k\cdot p$ 2-Band model, Physical Review B **103**, 205411 (2021), arXiv:2009.11301 [cond-mat].

[5] Y.-R. Wu, X.-F. Zhang, C.-F. Liu, W.-M. Liu, and Y.-C. Zhang, Superfluid density and collective modes of fermion superfluid in dice lattice, Scientific Reports **11**, 13572 (2021).

[6] J. Kang, T. Oh, J. Lee, and B.-J. Yang, Quantum geometric bound for saturated ferromagnetism (2024), arXiv:2402.07171 [cond-mat].

[7] J. Yu, C. J. Ciccarino, R. Bianco, I. Errea, P. Narang, and B. A. Bernevig, Non-trivial quantum geometry and the strength of electron–phonon coupling, Nature Physics **20**, 1262 (2024).
[8] T. Mitra, Electron-phonon interaction in the modified tight-binding approximation, Journal of Physics C: Solid State Physics **2**, 52 (1969).
[9] W. L. McMillan, Transition temperature of strong-coupled superconductors, Phys. Rev. **167**, 331 (1968).
[10] K. Sun, Z. Gu, H. Katsura, and S. Das Sarma, Nearly flatbands with nontrivial topology, Phys. Rev. Lett. **106**, 236803 (2011).
[11] N. Regnault and B. A. Bernevig, Fractional chern insulator, Physical Review X **1**, 021014 (2011).